Terpenoids, steroids and tocopherols in the organic matter of the Ob Fen (Western Siberia)

Andrey A. Grinko[1], Tatyana V. Cheshkova[2,3], Oleg G. Savichev[4], Elena V. Gershelis[1], Alexander D. Egorov[1]

[1] Sirius University, FT Sirius, Russia
[2] Institute of Petroleum Chemistry SB RAS, Tomsk, Russia
[3] Siberian State Medical University, Tomsk, Russia
[4] Tomsk Polytechnic University, Tomsk, Russia

SUMMARY

We present data on the composition and distribution of three significant components of peat organic matter (terpenoids, steroids and tocopherols) from two boreholes (H2 and H3) in the Ob Fen in Western Siberia. H2 is located closer to the edge of the peatland than H3. For borehole H2 it is shown that terpenoids and steroids are unevenly distributed along the borehole (up to 6 m depth) and their concentrations reach maxima at 0.50–0.75 m and 0.25–0.50 m, respectively. The spectrum of terpenoid and steroid components becomes broader with increasing sampling depth. The concentration of tocopherols is lower than the content of terpenoids and steroids. An uneven distribution of these components is also evident at different depths within borehole H3 (up to 5.0 m). These components generally decrease significantly in concentration with increasing depth, particularly below 2.75 m. The peat formation regime and organic matter composition differ between H2 and H3.

KEY WORDS: GC-MS, peatland, polycyclic compounds, pharmaceuticals, River Ob, river valley mire

INTRODUCTION

Peatlands play a major role in the functioning of regional and global biogeochemical cycles. During the formation of peatlands, some substances are intensively accumulated, transformed or removed, and this determines the important role of these ecosystems in the main biogeochemical (carbon, nitrogen, etc.) cycles (Limpens *et al.* 2008, Savichev *et al*. 2019). For example, their role in the carbon cycle varies with the quality of the organic matter (OM) in the peat and its chemical composition, as well as with its degree of decomposition (Wilson *et al.* 2022). From the point of view of industrial development of wetlands and control of their ecological state, the assessment of anthropogenic impact through monitoring of the degree of pollution and the capacity for self-remediation is mandatory (Russkikh *et al*. 2020, Savichev *et al*. 2022, Newman *et al*. 2023). Therefore, research that aims to study the composition of the peat and water in peatlands is of great importance (Matveenko *et al*. 2015, Duchko 2016, Serebrennikova *et al*. 2016, Savichev *et al*. 2018).

Peat is a complex multi-component system. Its formation and composition are influenced by physical, chemical and biological factors such as temperature, moisture, acidity and initial composition of the plant material, amongst others. These factors vary spatially within the peat body and thus have a significant influence on the accumulation of OM, its composition and the degree of its transformation (Orlov *et al.* 1996, Pancost *et al.* 2002, Kudeyarova 2006, Savichev *et al.* 2016). In this sense, spatial variation in the composition of OM allows us to trace the sources and conditions of peat formation (Kudeyarova 2006, Semyonov *et al*. 2006, Duchko *et al*. 2013).

Amongst the most important components of organic matter in peat are polycyclic compounds - terpenoids (triterpenoids) and steroids - which are products of incomplete decomposition of organic matter of plant and animal origin as a result of the activity of eukaryotic and bacterial organisms in peat-forming plant matter and, thus, directly linked to the carbon balance of the peatland ecosystem (López-Días *et al*. 2010, Serebrennikova *et al*. 2016, Talbot *et al*. 2016). Terpenoids are organic compounds that are derivatives of terpenes and are active participants in the metabolic processes of plants, including those growing on peat deposits. At the same time they have a wide spectrum of biological activity, and are thus

of potential interest for the development of new approaches to their use in pharmacology. Steroids are substances of eukaryotes (animal or plant origin), also with high biological activity. They are formed under natural conditions from isoprenoid precursors (Semyonov *et al.* 2006, Savicheva & Inisheva 2008). Tocopherols are natural compounds of plant origin belonging to a different class of organic compounds (methylated phenols) within the vitamin E family (Ahsan *et al*. 2015, Szewczyk *et al*. 2021). All of these components can be detected by gas chromatography - mass spectrometry (GC-MS) analysis and are common in peat systems, for example as compounds with the taraxerane skeleton and the oleanane skeleton, and as various steroids (Pancost *et al*. 2002).

The aim of this study was to determine the composition of polycyclic compounds in peat collected from an unpolluted ('background') section of the extensive Ob peatland in Western Siberia, counting terpenoids, steroids and tocopherols separately, and taking into account the contaminants detected. The objective was to identify regularities and peculiarities in the composition of terpenoid and steroidal components. In this way we aimed to gain new insights about the formation, evolution and chemical composition of the peat, and thus to deepen our understanding of the functioning of the Ob peatland ecosystem and its role in regional environmental changes (Savichev *et al*. 2013).

Figure 1. Positions of our five coring locations in the Ob Fen (Yandex Map). The cores discussed in this article are H2 (closer to the edge of the peatland) and H3 (closer to the centre).

METHODS

The Ob Fen is an extensive pristine river valley mire (Schipper *et al*. 2007) located in the Tomsk Region of Western Siberia (Savichev *et al*. 2013, Grinko *et al.* 2025), and one of the largest peatland ecosystems in the world. It stretches for about 100 km along the left bank of the Ob River valley in the form of a strip 2–5 km wide and up to 6+ m deep (Savichev *et al.* 2022). Peat samples were collected from a 'background' section of the peatland (without obvious signs of pollution) near the village of Nashekovo, Tomsk Oblast (56° 31′ 40″ N, 84° 03′ 40″ E). The study area and sampling methodology are described in detail by Savichev *et al*. (2013, 2022) and Grinko *et al*. (2025).

The peat samples were obtained from two boreholes (H2 and H3 in Figure 1) approximately 100 m apart, with H2 (56° 30.864' N, 84° 1.504' E) being closer to the edge of the peatland than H3 (56° 30.861′ N, 84° 1.565′ E). Some key characteristics of the peat profile are shown in Figure 2. Samples were collected along the whole depth of both boreholes, from 0 m to 6.0 m depth at H2 and from 0 m to 5.0 m depth at H3. The peat samples were sent to the laboratory immediately after collection and stored in a freezer at -20 °C. Grinko *et al.* (2025) provide a detailed characterisation of the H2 samples along with the full methodology for isolation and analysis of OM. Briefly, bitumoid was extracted from the peat samples with chloroform, separated into polar and non-polar fractions and analysed by GC-MS. The GC-MS analysis was performed on an Agilent 7890B (GC) - Agilent Q-TOF 7200 (MS) instrument using a DB-5ms quartz capillary column of length 30 m, inner diameter 0.25 mm and phase layer thickness 0.25 μm. The inlet temperature was 300 °C. The initial temperature of the column thermostat oven was 40 °C, rising at a rate of 5 °C min^{-1} to 150 °C then at 3 °C min^{-1} to 310 °C before holding constant at that temperature for 20 min. The flow rate of the carrier gas (helium) was 1.1 mL min^{-1}. Identification of compounds was based on the time of their yield on the column, as well as on the analysis of mass spectra of parent and fragment ions in Scan and SIM modes, using NIST 14 libraries and literature data. Quantitative calculations were performed using standards (hopanes) provided by Chiron AS, Norway.

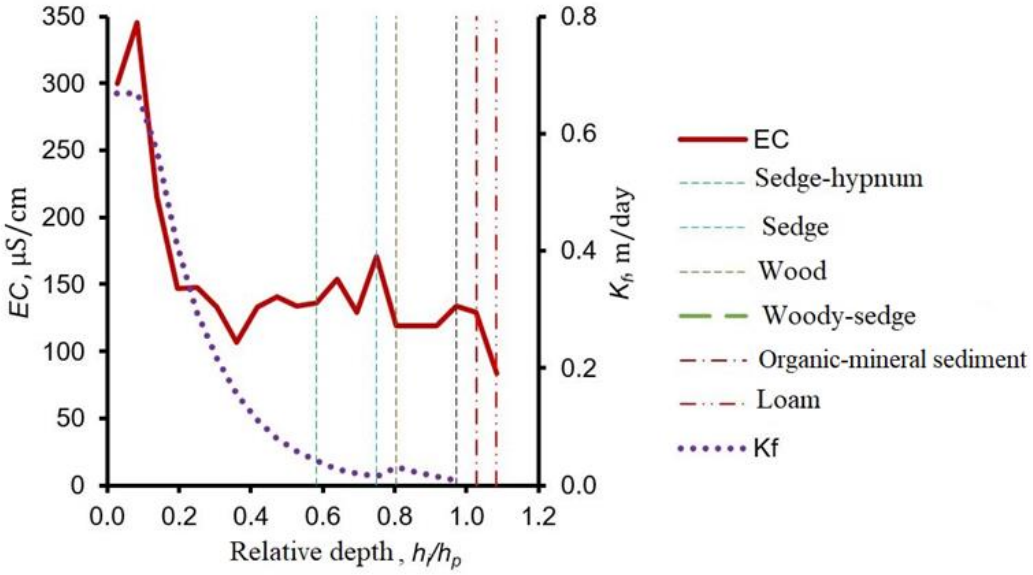

Figure 2. Variation of measured values of specific electrical conductivity (EC) and calculated values of the filtration coefficient (hydraulic conductivity; K_f) of peat in the vicinity of borehole H3 (from Savichev *et al.* 2022). The depths of peat type transitions in the profile are also shown.

RESULTS

The peat samples are characterised briefly in Table 1. The 191 m/z mass-fragmentograms and identified terpenoid and steroid components for peat at depths 0–0.25 m, 0.25–0.5 m, 0.5–0.75 m and 2.5–2.75 m in both cores, plus one or two basal samples (5.5–6 m depth in H2, 4.5–4.75 and 4.75–5 m depth in H3) are shown in Appendix 1. In both boreholes, the smallest number of compounds is found in the surface layer (Table 2). Below a sampling depth of 0.5 m the spectrum of terpenoid components expands. In core H2 the number of compounds continues to increase, sample by sample, to the base of the core. An interesting difference in borehole H3 is that the highest number of identified compounds (32) occurs at the 0.25–0.50 and 0.50–0.75 m levels, and the spectrum of terpenoids and steroids does not continue to increase with depth thereafter.

Figure 3 shows the main trends in the concentrations of total tocopherols, steroids and terpenoids along the two cores. In core H2, the concentration of tocopherols does not change much with depth, although a minimum is observed in the 2.50–2.75 m peat layer. On the other hand, the concentrations of steroids and terpenoids pass through maxima at depths of 0.25–0.50 m and 0.50–0.75 m, respectively, indicating a higher degree of diagenetic processing of peat OM at these levels. Betulin, a substance found in birch bark (which gives the bark a white colour), was detected in all samples (traces in H2-23 and H2-25), with a maximum in the

Table 1. Characterisation of peat samples collected in boreholes H2 and H3.

Depth (m)	Chloroform bitumoid yield (% dw)		Moisture (% dw)	
	H2	H3	H2	H3
0.00–0.25	8.32	14.07	92.38	84.85
0.25–0.50	17.35	8.79	90.15	89.33
0.50–0.75	10.22	3.68	82.73	89.21
2.50–2.75	4.92	6.48	78.57	81.46
4.50–4.75	-	0.79	-	63.19
4.75–5.00	-	1.57	-	28.48
5.50–6.00	1.29	-	30.62	-

Table 2. Number of compounds identified by GC-MS in analysed samples (mass-fragmentogram m/z 191).

Sample depth (m)	Core	
	H2	H3
0.00–0.25	7	14
0.25–0.50	14	32
0.50–0.75	24	32
2.50–2.75	21	23
4.50–4.75	-	20
4.75–5.00	-	18
5.50–6.00	27	-

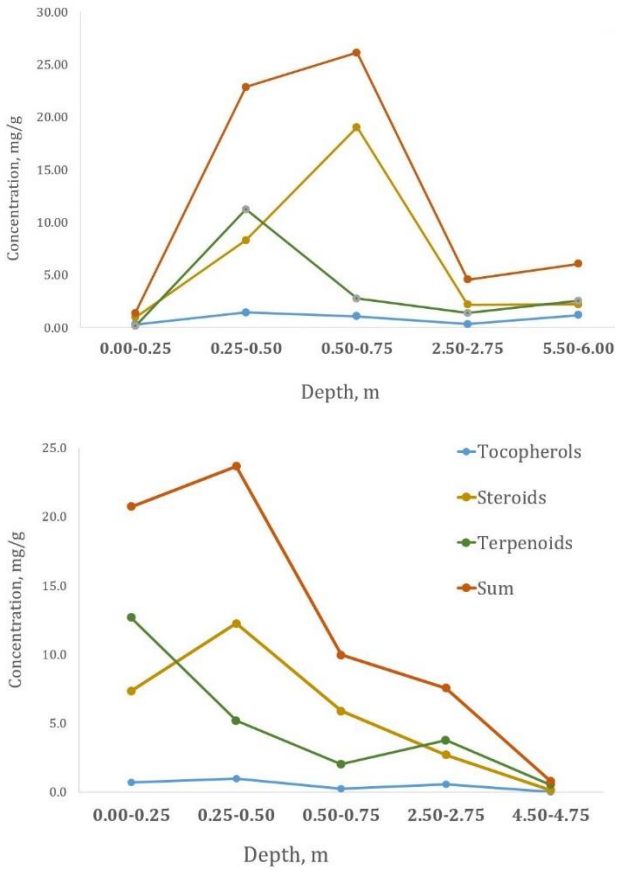

Figure 3. Distribution of the sum (red) of tocopherols (blue), steroids (brown) and terpenoids (green) with depth in the H2 (above) and H3 (below) boreholes. Contaminants are excluded.

0.25–0.50 m layer. Total compounds (excluding contaminants) also pass through maxima at the 0.20–0.50 and 0.50–0.75 m levels. Although the spectrum of steroids and terpenoids is broadest towards the deepest core depth, their maximum amounts are still in the depth interval 0.25–0.75 m. In contrast, in core H3 the local maximum for steroids is observed at 0.25–0.50 m and in general the concentrations of all identified components decrease with increasing sampling depth (Grinko *et al*. 2025), although there is a local maximum for triterpenoids at 2.50–2.75 m.

The structural formulae of the compounds identified in each core are summarised in Appendix 2. The source of the aromatic hydrocarbons DNP and NDUT appears to be peat plant matter (Smith 1990, Patel *et al*. 2020), while TMBA and iTMBA are most likely to be pyrogenic (Crnkovic *et al.* 2020). Of the 39 compounds identified, 30 are common to both cores whilst three occur in core H2 only and six in core H3 only. Three of the compounds found only in H3 also originate from peatland plant matter; although 2,3-dihydro-3,6-dimethylanthra[2,3-b]furan-4,11-dione is also believed to be the product of microbial transformation of synthetic contaminants. 2-pentacosanone and tridecyl decanoate (found in H3 only at depth 0.25–0.50 m and 0.50–0.75 m) may be contaminants derived from household reagents and cosmetics, and 2-benzylnaphthalene is apparently a combustion product of petroleum origin which is found only in upper layers (depth range 0.25–0.75 m). Concentration of the latter compound (~1.2 ng g^{-1}) was detected at the 0.25–0.50 m level. Conversely, 2-pentacosanone and tridecyl decanoate are not necessarily contaminants introduced from outside. 2-Pentacosanone is found in various plants because long-chain ketones are part of their cuticular waxes (Bianchi 1995, Kunst & Samuels 2003). Tridecyl decanoate may be related to anthropogenic loads in aquatic ecosystems (cosmetics, personal care products), but at the same time it is not considered to be a high-priority contaminant (Serrano *et al*. 2011, Yang *et al*. 2017).

DISCUSSION

The process of peat formation and transformation is extremely complex, in terms of both general biogeochemical and hydrological processes and specific details of peat formation and accumulation of transformation products in the peat deposit. Thus, describing peat formation processes in the Ob peatlands of south-eastern West Siberia is a complex multidimensional task, and we do not yet have a complete explanation of the mechanisms and conditions of peat formation. However, the data we have obtained show that, even in the absence of pronounced anthropogenic influence, there have been repeated significant changes in the conditions of peat formation in the past. This is a reliable fact that has been confirmed by other methods (Liss *et al*. 2001, Savichev 2024).

The expansion of terpenoid components in the peat below 0.5 m depth in core H2 appears to be associated with increased anaerobic microbial activity and a higher degree of diagenetic processing of OM, which generally continues to increase with increasing depth until the base of the deposit is reached. Although core H3 was only around 100 m farther from the edge of the mire, intensive microbial processing, which is associated with the input of relatively fresh OM, was confined to the relatively shallow depth range of 0.25–0.75 m in this core. Thus, despite the short distance between the boreholes, they have different OM accumulation and transformation regimes. We may also expect that

they have different hydrological regimes, because borehole H2 is located at the edge of the wetland area.

A difference in OM accumulation between central (H3) and edge (H2) locations within the study area has also been demonstrated. In general, a decrease in the concentrations of identified compounds was observed in the central borehole H3, while local maxima were observed closer to the edge of the peatland (borehole H2). This indicates different peat formation regimes.

Although the investigated area of the Ob Fen has not been subject to serious anthropogenic pollution, contaminants were found. The fact that 2-benzylnaphthalene was not detected in the surface layer suggests that it was carried into the peat profile by water movement. It is also worth noting that 2-benzylnaphthalene was not found in borehole H2 at the edge of the bog. The largest quantity of contaminants was found in the 0.25–0.50 m layer, indicating indirectly that these compounds are carried mainly by water movement bypassing the surface layer. At the same time, their further migration is limited to this layer by the low filtration coefficient (hydraulic conductivity) of deeper peat (Figure 2). Thus, they were concentrated in the near-surface sediment layer, suggesting that this layer acts as a filter. A significant decrease in all identified components occurs below the 2.75 m level, suggesting the presence of a geochemical barrier (Savichev *et al*. 2020).

Potential source for pharmaceutical components

In addition to qualitative and quantitative analyses of peat organic matter samples, we examined their potential as a source of bioactive substances. Tocopherols exhibit vitamin E activity in animals, functioning as potent fat-soluble antioxidants that protect cell membranes from free radical damage. Low plasma vitamin E levels are strongly associated with first-trimester miscarriage in women, and dietary vitamin E supplementation reduces miscarriage rates by approximately 50 % (Shamim *et al.* 2015). Vitamin E supplementation also improves lipid profiles in diabetes mellitus patients (Mohammad *et al.* 2021). This evidence underscores the importance of adequate vitamin E intake. Peat organic matter is comparable to industrial sources of natural tocopherols such as rice bran oil distillate, sunflower oil distillate, and palm oil fatty acid distillate.

Another major component, γ-sitosterol, demonstrates antidiabetic activity by reducing blood glucose and glycosylated hemoglobin in streptozotocin-induced diabetic models (Balamurugan *et al.* 2011). Betulin, a natural triterpenoid found in significant quantities in peat organic matter, is known for its protective effects against cardiovascular diseases and diabetes. Specifically, betulin potentiates insulin-stimulated glucose absorption by increasing PPARγ activity (Ko *et al.* 2016). In high-fat diet-fed C57BL/6J mice, betulin treatment improved insulin sensitivity and glucose tolerance by inhibiting SREBP expression. Furthermore, dietary supplementation with betulin reduced atherosclerotic plaque size and enhanced plaque stability (Tang *et al.* 2011). These findings highlight the therapeutic potential of peat-derived molecules for metabolic diseases like diabetes mellitus.

ACKNOWLEDGEMENTS

This work was supported by the grant of the state program of the «Sirius» Federal Territory «Scientific and technological development of the «Sirius» Federal Territory» (Agreement №18-03 date 10.09.2024).

AUTHOR CONTRIBUTIONS

AAG: initiation and organisation of work, performance of analyses, processing of results, manuscript writing; TVC: work with peat samples, methodological support, collection of analytical data; OGS: data interpretation, manuscript writing; EVG: organisation, administrative support and coordination of work; ADE: data interpretation, manuscript writing.

REFERENCES

Ahsan, H., Ahad, A., Siddiqui, W.A. (2015) A review of characterization of tocotrienols from plant oils and foods. *Journal of Chemical Biol*ogy, 8, 45–59.

Balamurugan, R., Duraipandiyan, V., Ignacimuthu, S. (2011) Antidiabetic activity of γ-sitosterol isolated from *Lippia nodiflora* L. in streptozotocin induced diabetic rats. *European Journal of Pharmacology*, 667(1–3), 410–418.

Bianchi, G. (1995) Plant waxes. In: Hamilton, R.J. (ed.) *Waxes: Chemistry, Molecular Biology and Functions*, The Oily Press, Dundee, 175–222.

Crnković, D., Sekulić, Z., Antonvić, D., Marinković, A., Popović, S., Nikolić, J., Drmanić, S. (2020) Origins of polycyclic aromatic hydrocarbons in sediments from the Danube and Sava Rivers and their tributaries in Serbia. *Polish Journal of Environmental Stud*ies, 29(3), 2101–2110.

Duchko, M.A. (2016) *Geokhimiya biomarkerov v torfakh yugo-vostochnoy chasti Zapadnoy Sibiri* (*Geochemistry of Biomarkers in Peats of the South-Eastern Part of Western Siberia*). Dissertation for the degree of Candidate of Geological and Mineralogical Sciences, Tomsk Polytechnic University Publishing House, 149 pp. (in Russian).

Duchko, M.A., Gulaya, E.V., Serebrennikova, O.V., Strelnikova, E.B., Preis, Yu.I. (2013) Raspredeleniye n-alkanov, steroidov i triterpenoidov v torfe i rasteniyakh bolota Tomnoye (Distribution of n-alkanes, steroids and triterpenoids in peat and plants of the Temnoe bog). *Bulletin of the Tomsk Polytechnic University*, 323(1), 40–44 (in Russian).

Grinko, A.A., Savichev, O.G., Cheshkova, T.V., Moiseeva, Yu.A., Gershelis, E.V. (2025) Organic matter in water and peat of the Ob Fen, Western Siberia. *Mires and Peat*, 32, 18, 24 pp.

Ko, B.-S., Kang, S., Moon, B.R., Ryuk, J.A., Park, S. (2016) A 70% ethanol extract of mistletoe rich in betulin, betulinic acid, and oleanolic acid potentiated β-cell function and mass and enhanced hepatic insulin sensitivity. *Evidence-Based Complementary and Alternative Medicine*, 2016, 7836823, 13 pp.

Kudeyarova A.Yu. (2006) O prirode i mekhanizmakh transformatsii gumusovykh veshchestv: kontseptual'nyye i prostranstvenno-vremennyye aspekty, Pochvennyye protsessy i prostranstvenno-vremennaya organizatsiya pochv (*On the Nature and Mechanisms of Transformation of Humus Substances: Conceptual and Spatial-Temporal Aspects, Soil Processes and Spatial-Temporal Organisation of Soils*). Nauka, Moscow, 212–229 (in Russian).

Kunst, L., Samuels, A.L. (2003) Biosynthesis and secretion of plant cuticular wax. *Progress in Lipid Research*, 42, 51–80.

Limpens, J., Berendse, F., Blodau, C., Canadell, J.G., Freeman, C., Holden, J., Roulet, N., Rydin, H., Schaepman-Strub, G. (2008) Peatlands and the carbon cycle: from local processes to global implications - a synthesis. *Biogeosciences*, 5, 1475–1491.

Liss, O.L., Abramova, L.I., Avetov, N.A., Berezina, N.A., Inisheva, L.I., Kurnishkova, T.V., Sluka, Z.A., Tolpysheva, T.Y., Shvedchikova N.K. (2001) Bolotnyye sistemy Zapadnoy Sibiri i ikh prirodookhrannoye znacheniye (*Swamp Systems of Western Siberia and their Nature Conservation Value*). Grif and K, Tula, 584 pp. (in Russian).

López-Días, V., Borrego, A.G., Blanco, C.G., Arboleya, M., López-Sáez, J.A., López-Merino, L. (2010) Biomarkers in a peat deposit in Northern Spain (Huelga de Bayas, Asturias) as proxy for climate variation. *Journal of Chromatography A*, 1217, 3538–3546.

Matveenko, I.A., Savichev, O.G., Bazanov, V.A., Ivanova, Ye.V. (2015) Spatial-temporal regularities in changing chemical composition of bog waters in taiga zone of Western Siberia. *Procedia Chemistry*, 15, 206–212.

Mohammad, A., Falahi, E., Barakatun-Nisak, M.Y., Hanipah, Z.N., Redzwan, S.M., Yusof, L.M., Gheitasvand, M., Rezaie, F. (2021) Systematic review and meta-analyses of vitamin E (alpha-tocopherol) supplementation and blood lipid parameters in patients with diabetes mellitus. *Diabetes & Metabolic Syndrome: Clinical Research & Reviews*, 15(4), 102158, 10 pp.

Newman, J.E., Levasseur, P.A., Beckett, P., Watmough, S.A. (2023) The impact of severe pollution from smelter emissions on carbon and metal accumulation in peatlands in Ontario, Canada. *Environmental Pollution*, 320, 121102, 11 pp.

Orlov, D.S., Biryukova, O.G., Sukhanova, N.I. (1996) *Organicheskoye veshchestvo pochv Rossiyskoy Federatsii* (*Organic Substance of Soils of the Russian Federation*.) Nauka, Moscow, 256 pp. (in Russian).

Pancost, R.D., Baas, M., van Geel, B., Damste, J.S.S. (2002) Biomarkers as proxies for plant inputs to peats: an example from a sub-boreal ombrotrophic bog. *Organic Geochemistry*, 33, 675–690.

Patel, A.B., Shaikh, S., Jain, K.R., Desai, C., Madamwar, D. (2020) Polycyclic aromatic hydrocarbons: Sources, toxicity, and remediation approaches. *Frontiers in Microbiology*, 11, 562813, 23 pp.

Russkikh, I.V., Strelnikova, E.B., Serebrennikova, O.V., Voistinova, E.S., Kharangevskaya, Y.A. (2020) Identification of hydrocarbons in the waters of bogs of the southern taiga of Western Siberia. *Geochemistry International*, 65(4), 405–414.

Savichev O.G. (2024) Izmeneniya usloviy vzaimodeystviya podzemnykh, rechnykh i bolotnykh vod pri zabolachivanii Zapadno-Sibirskoy ravniny v golotsene (Changes in the conditions of interaction between ground, river and swamp water during waterlogging of the West Siberian Plain in the Holocene). *Bulletin of the Tomsk Polytechnic University, Geo Assets Engineering*, 335(2), 170–186 (in Russian).

Savichev, O.G., Guseva, N.V., Kupriyanov, N.A., Skorokhodova, A.A., Akhmed-Ogly, K.V. (2013) Khimicheskiy sostav vod Obskogo bolota (Zapadnaya Sibir') i yego prostranstvennyye

izmeneniya pod vliyaniyem sbrosov zagryaznyayushchikh veshchestv (Chemical composition of Ob bog waters (Western Siberia) and its spatial changes under the influence of pollutant discharges). *Bulletin of the Tomsk Polytechnic University*, *Geo Assets Engineering*, 32 (1), 168–172 (in Russian).

Savichev, O.G., Mazurov, A.K., Semiletov, I.P., Bazanov, V.A., Guseva, N.V., Khvashchevskaya, A.A., Nalivajko, N.G. (2016) Gidrogeo-khimicheskiye usloviya formirovaniya oligotrofnykh bolotnykh ekosistem (Hydrogeo-chemical conditions for the formation of oligotrophic mire ecosystems). Izvestiya Rossiiskoi Akademii Nauk, Seriya Geograficheskaya (News of the Russian Academy of Sciences, Geographical series), 2016(5), 60–69. https://doi.org/10.15356/0373-2444-2016-5-60-69

Savichev, O.G., Mazurov, A.K., Rudmin, M.A., Khvashchevskaya, A.A., Dauletova, A.B. (2018) Izmeneniya khimicheskogo sostava kislotnykh vytyazhek po glubine torfyanoy zalezhi vnutribolotnykh ekosistem Vasyuganskogo bolota (Zapadnaya Sibir') (Changes in chemical composition of acid extracts on depth of peat deposit of the Vasyugan mire ecological systems (Western Siberia)). *Bulletin of the Tomsk Polytechnic University, Geo Assets Engineering,* 329(9), 101–116 (in Russian).

Savichev, O.G., Mazurov, A.K., Rudmin, M.A., Shakhova, N.E., Sergienko, V.I., Semiletov, I.P. (2019) Mechanisms of accumulation of chemical elements in a peat deposit in the eastern part of Vasyugan Swamp (West Siberia). *Doklady Earth Sciences*, 486(1), 568–570.

Savichev, O., Soldatova, E., Rudmin, M., Mazurov, A. (2020) Geochemical barriers in oligotrophic peat bog (Western Siberia). *Applied Geochemistry*, 113, 104519, 11 pp.

Savichev, O.G., Yang, H., Zhou, D. (2022) Gidrogeodinamicheskiye i gidrogeokhimicheskiye usloviya samoochishcheniya vod Obskogo bolota (Zapadnaya Sibir') (Hydrogeodynamic and hydrogeochemical conditions of self-purification of water of the Ob bog (Western Siberia)). *Bulletin of the Tomsk Polytechnic University, Geo Assets Engineering*, 333(4), 115–125 (in Russian).

Savicheva, O.G., Inisheva, L.I. (2008) Biochemical activity of the peat soil of a river marsh ecosystem, *Contemporary Problems of Ecology*, 6, 666–672.

Schipper, A.M., Zeefat, R., Tanneberger, F., Zuidam, J.P., Hahne, W., Schep, S.A., Loos, S., Bleuten, W., Joosten, H., Lapshina, E.D., Wassen, M.J. (2007) Vegetation characteristics and eco-hydrological processes in a pristine mire in the Ob River valley (Western Siberia). *Plant Ecology*, 193, 131–145.

Semyonov, V.M., Ivannikova, L.A., Kuznetsova, T.V. (2006) Strukturno-funktsional'noye sostoyaniye organicheskogo veshchestva pochvy. Pochvennyye protsessy i prostranstvenno-vremennaya organizatsiya pochv (*Structural and Functional State of Soil Organic Matter. Soil Processes and Spatial and Temporal Organisation of Soils*). Nauka, Moscow, 230–247 (in Russian).

Serebrennikova, O., Strelnikova, E., Preis, Y., Duchko, M., Rousskikh, I., Kaduchagov, P., Peresedova, A. (2016) The composition of biologically active compounds in peat from different climatic zones of Western Siberia. *MATEC Web of Conferences*, 85, 01006, 4 pp. https://doi.org /10.1051/matecconf/20168501006

Serrano, R., Mestre, J-N., Portoles, T., Amat, F., Hernandez, F. (2011) Non-target screening of organic contaminants in marine salts by gas chromatography coupled to high-resolution time-of-flight mass spectrometry. *Talanta*, 85, 877–884.

Shamim, A.A., Schulze, K., Merrill, R.D., Kabir, A., Christian, P., Shaikh, S., Wu, L., Ali, H., Labrique, A.B., Mehra, S., Klemm, R.D., Rashid, M., Sungpuag, P., Udomkesmalee, E., West, K.P.Jr. (2015) First-trimester plasma tocopherols are associated with risk of miscarriage in rural Bangladesh. *The American Journal of Clinical Nutrition*, 101(2), 294–301.

Smith, M.R. (1990) The biodegradation of aromatic hydrocarbons by bacteria. *Biodegradation*, 1(2–3), 191–206.

Szewczyk, K., Chojnacka, A., Górnicka, M. (2021) Tocopherols and tocotrienols—bioactive dietary compounds; What is certain, what is doubt? *International Journal of Molecular Sciences*, 22(12), 6222, 17 pp.

Talbot, H.M., McClymont, E.L., Inglis, G.N., Evershed, R.P., Pancost, R.D. (2016) Origin and preservation of bacteriohopanepolyol signatures in *Sphagnum* peat from Bissendorfer Moor (Germany). *Organic Geochemistry*, 97, 95–110.

Tang, J.J., Li, J.G., Qi, W., Qiu, W.W., Li, P.S., Li, B.L., Song, B.L. (2011) Inhibition of SREBP by a small molecule, betulin, improves hyperlipidemia and insulin resistance and reduces atherosclerotic plaques. *Cell Metabolism*, 13(1), 44–56.

Wilson, R.M., Hough, M.A., Verbeke, B.A., Hodgkins, S.B., Chanton, J.P., Saleska, S.D., Rich, V.I., Tfaily, M.M. (2022) Plant organic matter inputs exert a strong control on soil organic

matter decomposition in a thawing permafrost peatland. *Science of The Total Environment*, 820, 152757.

Yang, Y., Ok, Y.S., Kim, K-H., Kwon, E.E., Tsang, Y.F. (2017) Occurrences and removal of pharmaceuticals and personal care products (PPCPs) in drinking water and water/sewage treatment plants: A review. *Science of the Total Environment*, 596–597, 303–320.

Submitted 23 May 2024, final revision 29 Aug 2025
Editors: Olivia Bragg and Gerald Jurasinski

Author for correspondence: Andrey Alekseevich Grinko, International Centre for Ecology and Climate Change Research (ICECCR), Sirius University of Science and Technology, 1 Olimpiysky ave, 354340, FT Sirius, Russia. Tel: +7 8 (862) 241-98-44, ext. 5763; E-mail: andreyagrinko@gmail.com
Alexander Dmitrievich Egorov, Sirius University, FT Sirius, Russia. E-mail: egorov.ad@talantiuspeh.ru
Oleg Gennadievich Savichev, Tomsk Polytechnic University, Tomsk, Russia. E-mail: osavichev@mail.ru

Appendix 1

Table A1.1. Core H2, depth 0.00–0.25 m. Composition and content of identified steroid and terpenoid components of sample H2-23 by m/z 191. The labels on the mass fragmetogram are the peak numbers.

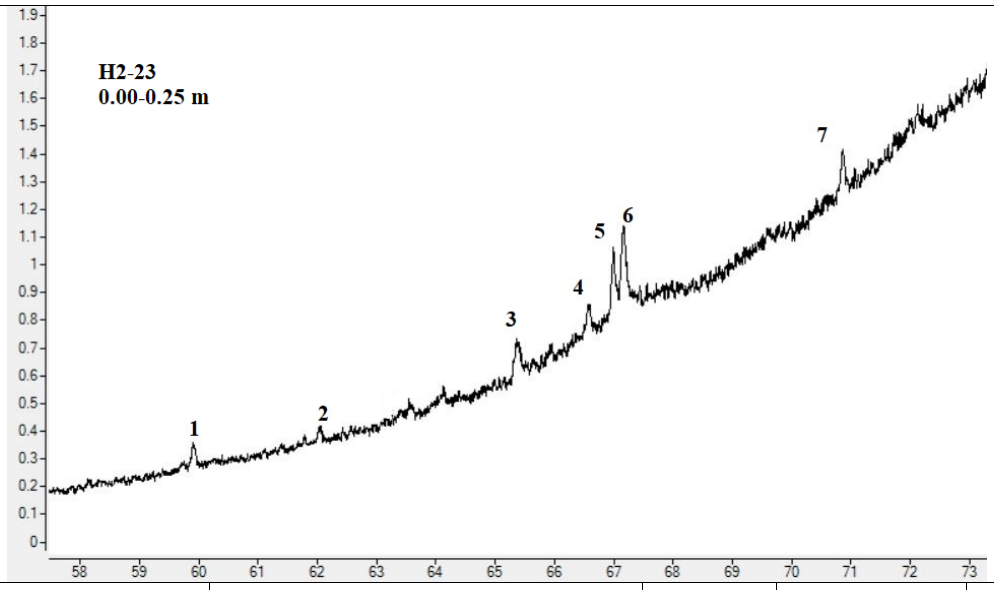

Peak No.	m/z	Component	Gross formula	Dry mass concentration (μg g^{-1})	Type
1	240,296, 341	Unknown compound	–	26.0	unknown
2	135,189, 191, 299	28-Nor-Δ12, Δ18-oleandien-3-ol	$C_{30}H_{52}O$	26.0	terpenoid
3	151, 191, 416	β-Tocopherol	$C_{29}H_{48}O_2$	290.0	vitamin E
4	315, 400	Campesterol	$C_{28}H_{48}O$	29.0	steroid
5	189, 191	Diploptene	$C_{30}H_{50}$	75.3	terpenoid
6	213, 329, 414	γ-Sitosterol	$C_{29}H_{50}O$	920.0	steroid
7	135, 189	Betulinaldehyde	$C_{30}H_{48}O_2$	29.0	terpenoid

Table A1.2. Core H2, depth 0.25–0.50 m. Composition and content of identified steroid and terpenoid components of sample H2-24 by m/z 191. The labels on the mass fragmetogram are the peak numbers.

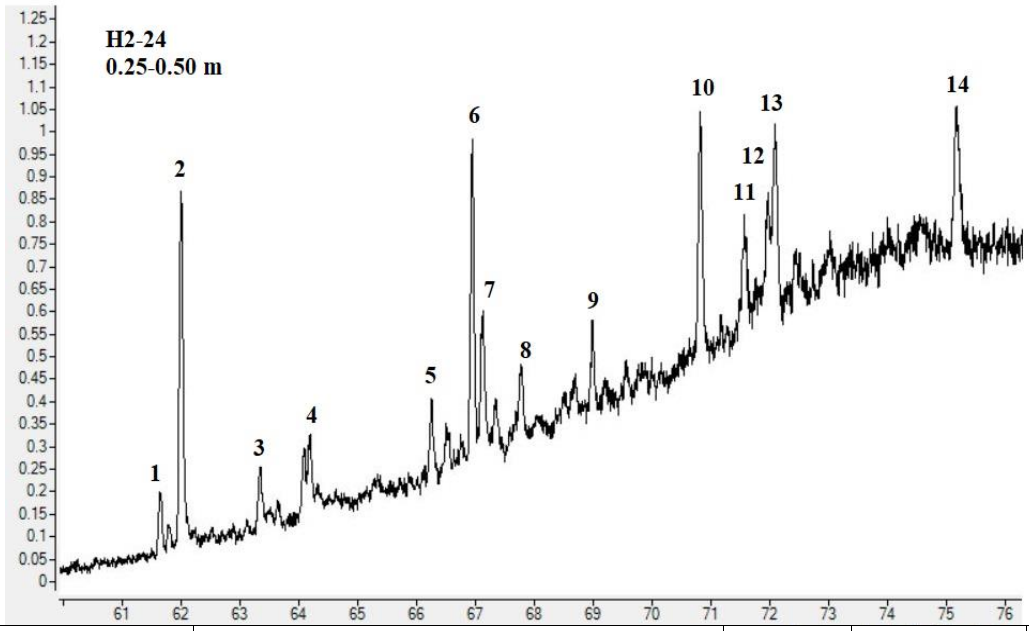

Peak No.	m/z	Component	Gross formula	Dry mass concentration (μg g^{-1})	Type
1	151, 191, 416	γ-Tocopherol	$C_{29}H_{48}O_2$	190.0	vitamin E
2	151, 191, 416	β-Tocopherol	$C_{29}H_{48}O_2$	1230.0	vitamin E
3	191, 215, 233, 373	(3β,5β)-Cholestan-3-ol,	$C_{27}H_{48}O$	137.1	steroid
4	251, 376	Ergosta-5,7,9(11),22-tetraen-3-ol, (3β,22E)	$C_{28}H_{42}O$	156.0	steroid
5	316, 444	Citrostediol	$C_{30}H_{52}O_2$	746.0	steroid
6	189, 191	Diploptene	$C_{30}H_{50}$	2047.0	terpenoid
7	213, 329, 414	γ-Sitosterol	$C_{29}H_{50}O$	5970,0	steroid
8	124, 229, 398	4-Campestene-3-one	$C_{28}H4_6O$	1260,0	steroid
9	191,397, 496	4,4-Dinorlupan-4-one-28-carboxylic acid, 3β-methyl-, methyl ester	$C_{30}H_{48}O_3$	271.1	terpenoid
10	189, 426	Lupeol	$C_{30}H_{50}O$	2630.0	terpenoid
11	175, 438	9,19-Cyclo-25,26-epoxyergostan-3-ol, 4,4,14-trimethyl-, acetate	$C_{33}H_{54}O_3$	1943.0	steroid
12	189, 191, 412	Olean-3-ol	$C_{30}H_{52}O$	727.2	terpenoid
13	189, 191, 470	18α-Olean-3β-ol, acetate	$C_{32}H_{54}O_2$	1440.0	terpenoid
14	189, 207, 411, 442	Betulin	$C_{30}H_{50}O_2$	4095.0	terpenoid

Table A1.3. Core H2, depth 0.50–0.75 m. Composition and content of identified steroid and terpenoid components of sample H2-25 by m/z 191. The labels on the mass-fragmentogram are the peak numbers.

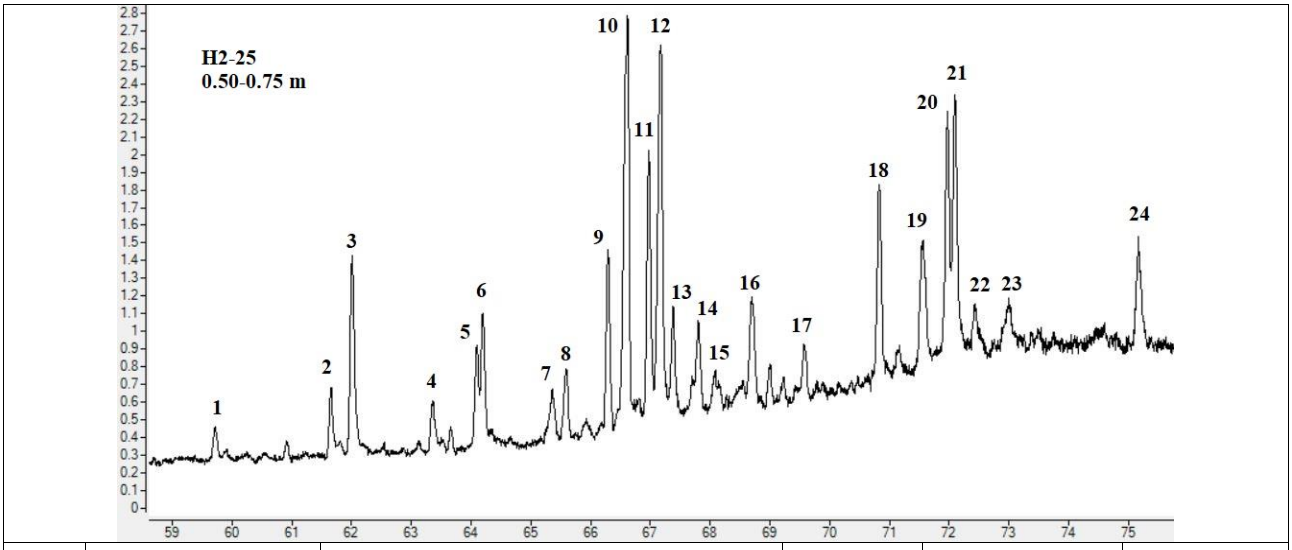

Peak No.	m/z	Component	Gross formula	Dry mass concentration (μg g^{-1})	Type
1	137, 177, 402	δ-Tocopherol	$C_{27}H_{46}O_2$	214.0	vitamin E
2	151, 191, 416	γ-Tocopherol	$C_{29}H_{48}O_2$	275.0	vitamin E
3	151, 191, 416	β-Tocopherol	$C_{29}H_{48}O_2$	562.0	vitamin E
4	215,233,373, 388	Cholestanol	$C_{27}H_{48}O$	235.0	steroid
5	121, 191	C_{28} 17β21β hopane	$C_{28}H_{48}$	143.0	terpenoid
6	255, 270	Trimethylbenz[a]anthracene **(TMBA)**	$C_{21}H_{18}$	0.014	aromatic HC
7	315, 400	Campesterol	$C_{28}H_{48}O$	1760.0	steroid
8	255, 270	Trimethylbenz(a)anthracene isomer **(iTMBA)**	$C_{21}H_{18}$	0.0052	aromatic HC
9	316, 444	Citrostediol	$C_{30}H_{52}O_2$	408.2	steroid
10	146, 378,	(22E)-Ergosta-3,5,7,22-tetraene	$C_{28}H_{42}$	4280.1	steroid
11	189, 191	Diploptene	$C_{30}H_{50}$	1328.0	terpenoid
12	213, 329, 414	γ-Sitosterol	$C_{29}H_{50}O$	6405.1	steroid
13	215, 233, 401	Stigmastanol	$C_{29}H_{52}O$	2012.0	steroid
14	124, 229, 398	4-Campestene-3-one	$C_{28}H_{46}O$	327.2	steroid
15	217, 231, 414	3-oxo-Stigmastane	$C_{29}H_{50}O$	1450.0	steroid
16	189,218, 426	α-Amyrin	$C_{30}H_{50}O$	643.1	terpenoid
17	124, 229, 289, 412	γ-Sitostenone	$C_{29}H_{48}O$	1603.0	steroid
18	189, 426	Lupeol	$C_{30}H_{50}O$	643.0	terpenoid
19	191, 396	4,4-Dimethylcholesterol	$C_{29}H_{50}O$	531.0	steroid
20	191	Unknown C_{35} homohopane	$C_{35}H_{62}$	418.0	terpenoid
21	191,470	18α-Olean-3β-ol, acetate	$C_{32}H_{54}O_2$	357.0	terpenoid
22	189, 426, 440	Homolupeol	$C_{31}H_{52}0$	265.2	terpenoid
23	395, 428	Lanost-8-en-3-ol, (3β)-	$C_{30}H_{52}O$	347.1	steroid
24	189, 207, 411, 442	Betulin	$C_{30}H_{50}O_2$	827.0	terpenoid

Table A1.4. Core H2, depth 2.50–2.75 m. Composition and content of identified steroid and terpenoid components of sample H2-33 by m/z 191. The labels on the mass fragmetogram are the peak numbers.

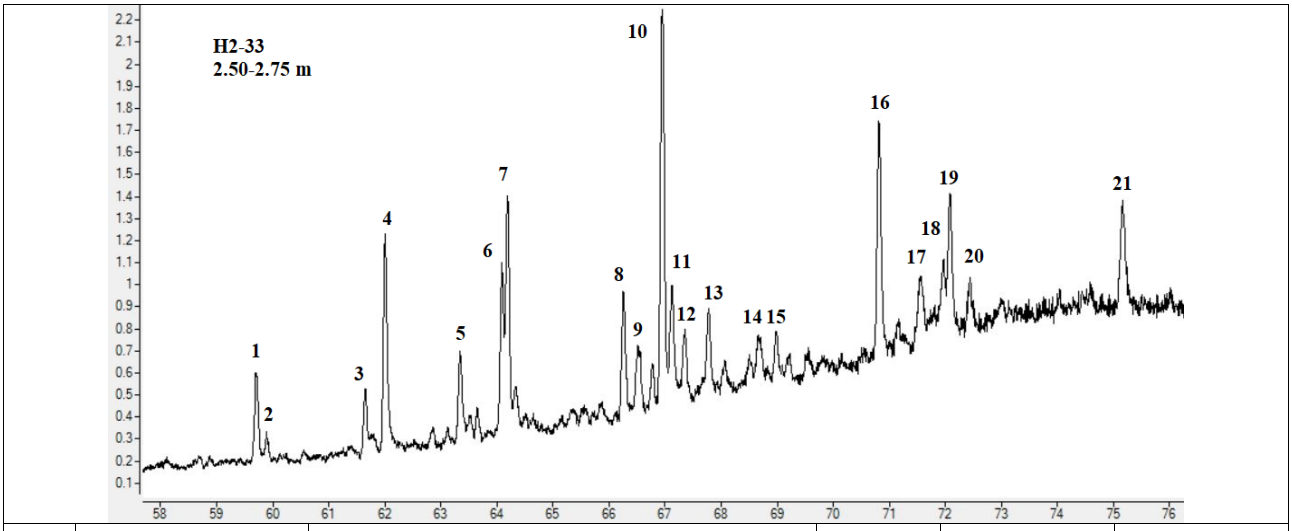

Peak No.	m/z	Component	Gross formula	Dry mass concentration (μg g^{-1})	Type
1	137, 177, 402	δ-Tocopherol	$C_{27}H_{46}O_2$	96.0	vitamin E
2	268, 296	Dinaphtho[2,3-b:1',2'-d]pyran-7-one **(DNP)**	$C_{21}H_{12}O_2$	0.00013	aromatic HC
3	151, 191, 416	γ-Tocopherol	$C_{29}H_{48}O_2$	74.2	vitamin E
4	151, 191, 416	β-Tocopherol	$C_{29}H_{48}O_2$	153.0	vitamin E
5	215,233,373, 388	Cholestanol	$C_{27}H_{48}O$	71.1	steroid
6	121, 191	C_{28} 17β21β hopane	$C_{28}H_{48}$	40.0	terpenoid
7	191, 218, 410	Olean-13(18)-ene	$C_{30}H_{50}$	57.0	terpenoid
8	316, 444	Citrostediol	$C_{30}H_{52}O_2$	149.0	steroid
9	145, 426	Naphthalene, 5-(1-decylundecyl)-1,2,3,4-tetrahydro- 9 **(NDUT)**	$C_{31}H_{54}$	0.00023	aromatic HC
10	189, 191	Diploptene	$C_{30}H_{50}$	248.0	terpenoid
11	213, 329, 414	γ-Sitosterol	$C_{29}H_{50}O$	858.0	steroid
12	215, 233, 401	Stigmastanol	$C_{29}H_{52}O$	694.0	steroid
13	124, 229, 398	4-Campestene-3-one	$C_{28}H_{46}O$	178.0	steroid
14	217, 231, 414	3-oxo-Stigmastane	$C_{29}H_{50}O$	95.0	steroid
15	259, 456	Unknown aromatic compound	–	0.00081	aromatic HC
16	189, 426	Lupeol	$C_{30}H_{50}O$	294.0	terpenoid
17	191, 396	4,4-Dimethylcholesterol	$C_{29}H_{50}O$	128.0	steroid
18	191	Unknown C_{35} homohopane	$C_{35}H_{62}$	46.1	terpenoid
19	191,470	18α-Olean-3β-ol, acetate	$C_{32}H_{54}O_2$	104.0	terpenoid
20	189, 207, 398	Betulinaldehyde	$C_{30}H_{48}O_2$	319.0	terpenoid
21	189, 207, 411, 442	Betulin	$C_{30}H_{50}O_2$	370.0	terpenoid

Table A1.5. Core H2, depth 5.50–6.00 m. Composition and content of identified steroid and terpenoid components of sample H2-45-46 by m/z 191. The labels on the mass fragmetogram are the peak numbers.

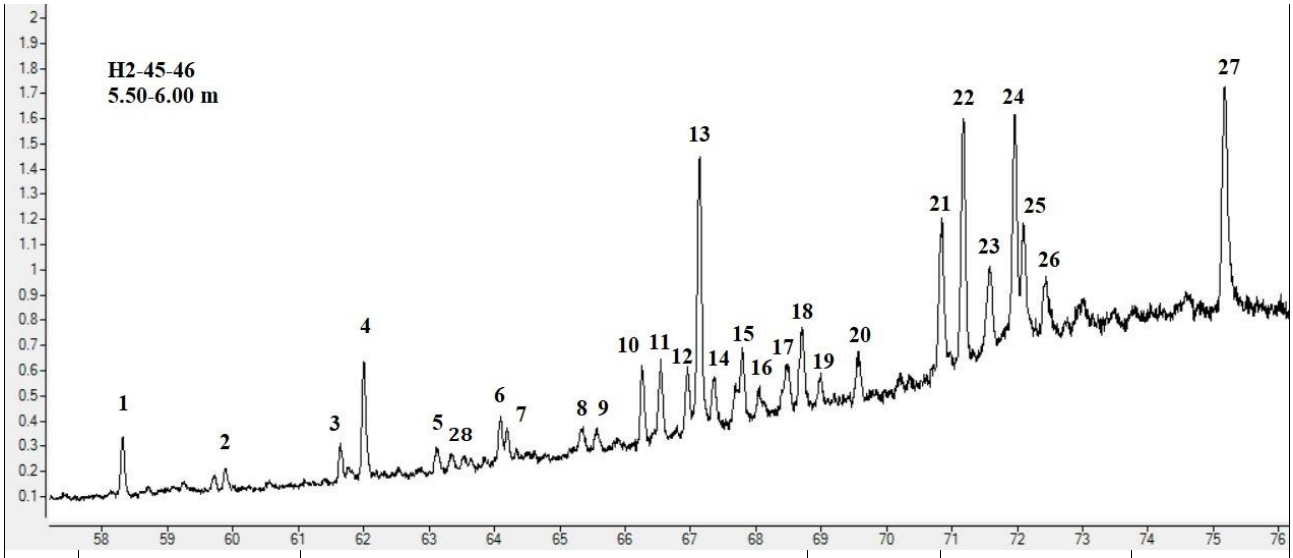

Peak No.	m/z	Component	Gross formula	Dry mass concentration (μg g^{-1})	Type
1	191, 384	17α,21β-28,30-Bisnorhopane	$C_{28}H_{48}$	180.0	terpenoid
2	137,177, 402	δ-Tocopherol	$C_{27}H_{46}O_2$	643.0	vitamin E
3	151,191, 416	γ-Tocopherol	$C_{29}H_{48}O_2$	205.0	vitamin E
4	151, 191, 416	β-Tocopherol	$C_{29}H_{48}O_2$	321.0	vitamin E
5	213,301, 386	Cholesterol	$C_{27}H_{46}O$	101.0	steroid
28	215,233,373, 388	Cholestanol	$C_{27}H_{48}O$	12.8	steroid
6	121, 191	C_{28} 17β21β hopane	$C_{28}H_{48}$	321.0	terpenoid
7	255, 270	Trimethylbenz[a]anthracene **(TMBA)**	$C_{21}H_{18}$	0.00064	aromatic HC
8	315, 400	Campesterol	$C_{28}H_{48}O$	41.1	steroid
9	255, 270	Trimethylbenz(a)anthracene isomer **(iTMBA)**	$C_{21}H_{18}$	0.00013	aromatic HC
10	316, 444	Citrostediol	$C_{30}H_{52}O_2$	33.4	steroid
11	146, 378,	(22E)-Ergosta-3,5,7,22-tetraene	$C_{28}H_{42}$	104.0	steroid
12	189, 191	Diploptene	$C_{30}H_{50}$	132.0	terpenoid
13	213, 329, 414	γ-Sitosterol	$C_{29}H_{50}O$	652.0	steroid
14	215, 233, 401	Stigmastanol	$C_{29}H_{52}O$	182.0	steroid
15	124, 229, 398	4-Campestene-3-one	$C_{28}H_{46}O$	60.1	steroid
16	217, 231, 414	3-oxo-Stigmastane	$C_{29}H_{50}O$	112.0	steroid
17	268, 385, 416	Unknown compound	–	74.6	unknown
18	189,218, 426	α-Amyrin	$C_{30}H_{50}O$	283.0	terpenoid
19	259, 456	Unknown compound	–	6.4	unknown
20	124, 229, 289, 412	γ-Sitostenone	$C_{29}H_{48}O$	189.0	steroid
21	189, 426	Lupeol	$C_{30}H_{50}O$	977.0	terpenoid
22	109, 273, 426	Friedelan-3-one	$C_{30}H_{50}O$	185.0	terpenoid

23	191, 396	4,4-Dimethylcholesterol	$C_{29}H_{50}O$	694.0	steroid
24	191	Unknown C_{35} homohopane	$C_{35}H_{62}$	41.1	terpenoid
25	191,470	18α-Olean-3β-ol, acetate	$C_{32}H_{54}O_2$	33.4	terpenoid
26	189, 207, 398	Betulinaldehyde	$C_{30}H_{48}O_2$	109.0	terpenoid
27	189, 207, 411, 442	Betulin	$C_{30}H_{50}O_2$	271.0	terpenoid

Table A1.6. Core H3, depth 0.00–0.25 m. Composition and content of identified steroid and terpenoid components of sample H3-67 by m/z 191. The labels on the mass fragmetogram are the peak numbers.

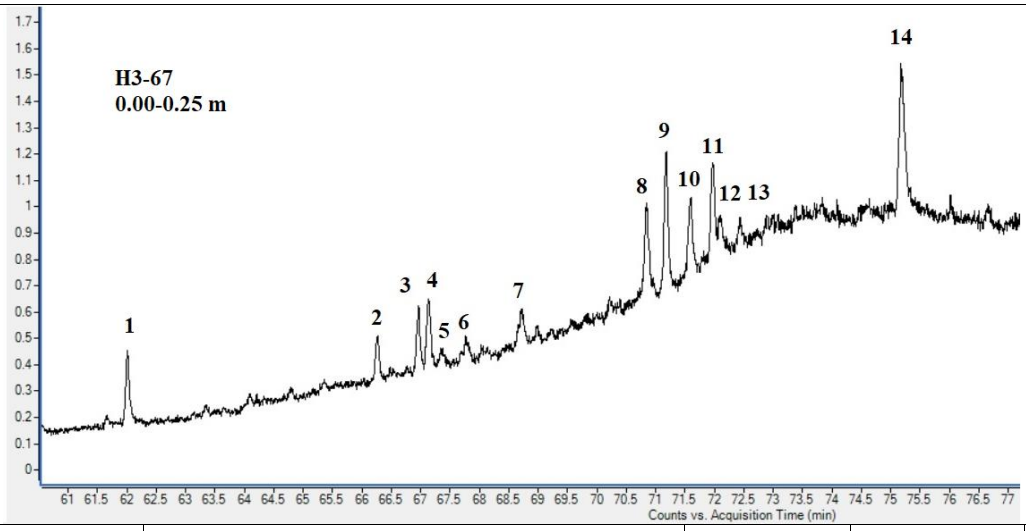

Peak No.	m/z	Component	Gross formula	Dry mass concentration (μg g^{-1})	Type
1	151, 191, 416	β-Tocopherol	$C_{29}H_{48}O_2$	703.0	vitamin E
2	316, 444	Citrostediol	$C_{30}H_{52}O_2$	529.0	steroid
3	189, 191	Diploptene	$C_{30}H_{50}$	763.0	terpenoid
4	213, 329, 414	γ-Sitosterol	$C_{29}H_{50}O$	4450.0	sreroid
5	215, 233, 401	Stigmastanol	$C_{29}H_{52}O$	1007.0	steroid
6	124, 229, 398	4-Campestene-3-one	$C_{28}H_{46}O$	382.0	steroid
7	191,397, 496	4,4-Dinorlupan-4-one-28-carboxylic acid, 3β-methyl-, methyl ester	$C_{30}H_{48}O_3$	3129.0	terpenoid
8	189, 411	Betulinaldehyde	$C_{30}H_{48}O_2$	1280.0	terpenoid
9	273, 411, 426	Friedelan-3-one	$C_{30}H_{50}O$	1892.0	terpenoid
10	175, 438	9,19-Cyclo-25,26-epoxyergostan-3-ol, 4,4,14-trimethyl-, acetate	$C_{33}H_{54}O_3$	1003.0	steroid
11	189, 191, 412	Olean-3-ol	$C_{30}H_{52}O$	521.0	terpenoid
12	189, 191, 470	18α-Olean-3β-ol, acetate	$C_{32}H_{54}O_2$	474.0	terpenoid
13	189, 426, 440	Homolupeol	$C_{31}H_{52}0$	293.1	terpenoid
14	189, 207, 411, 442	Betulin	$C_{30}H_{50}O_2$	4316.1	terpenoid

Table A1.7. Core H3, depth 0.25–0.50 m. Composition and content of identified steroid and terpenoid components of sample H3-68 by m/z 191. The labels on the mass fragmetogram are the peak numbers.

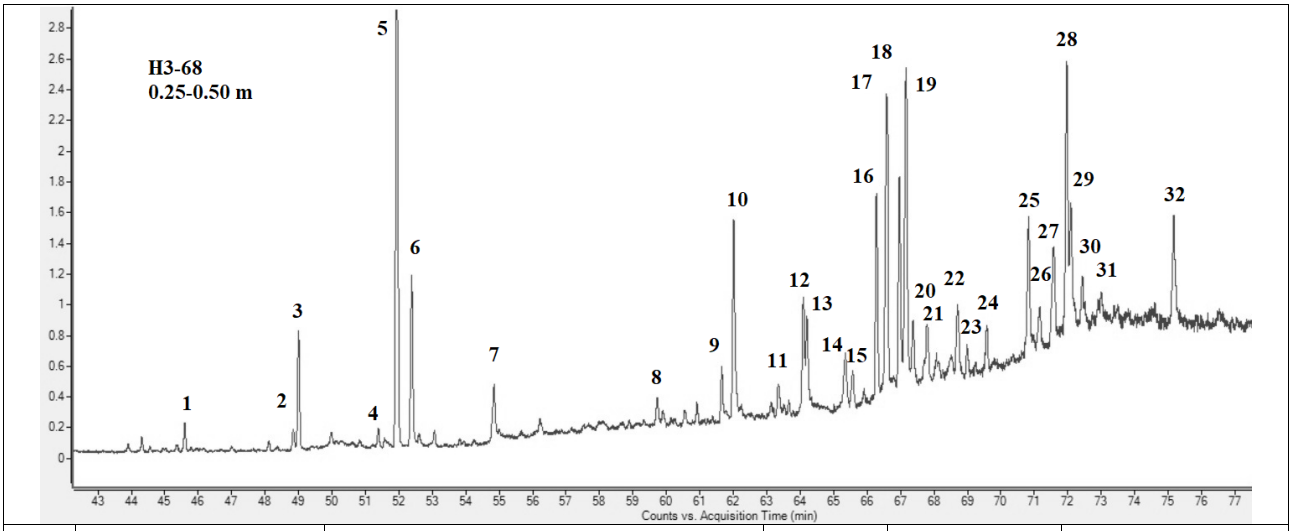

Peak No.	m/z	Component	Gross formula	Dry mass concentration (μg g^{-1})	Type
1	199, 281	Unknown compound	–	20.30	unknown
2	145,159, 294	Unknown compound	–	15.20	unknown
3	207, 263, 278	Anthra[2,3-b]furan-4,11-dione, 2,3-dihydro-3,6-dimethyl-	$C_{18}H_{14}O_3$	0.00016	aromatic HC
4	129, 173	Tridecyl decanoate	$C_{23}H_{46}O_2$	0.16	ester
5	121, 219, 330	Pregnane-3,11,20-trione, (5β)-	$C_{21}H_{30}O_3$	1241.0	steroid
6	202, 218	2-Benzylnaphthalene	$C_{17}H_{14}$	0.0012	aromatic contaminant (from petroleum products)
7	51, 96, 366	2-Pentacosanone	$C_{25}H_{50}O$	11.60	ketone
8	137, 177, 402	δ-Tocopherol	$C_{27}H_{46}O_2$	243.0	vitamin E
9	151, 191, 416	γ-Tocopherol	$C_{29}H_{48}O_2$	95.1	vitamin E
10	151, 191, 416	β-Tocopherol	$C_{29}H_{48}O_2$	650.0	vitamin E
11	215,233,37,388	Cholestanol	$C_{27}H_{48}O$	74.1	steroid
12	121, 191	C_{28} β-hopane	$C_{28}H_{48}$	414.2	hopanoid
13	203, 2017	24-Noroleana-4(23),12-diene, 3-methyl-, (3α)-	$C_{30}H_{48}$	130.0	terpenoid
14	315, 400	Campesterol	$C_{28}H_{48}O$	1616.0	steroid
15	255, 270	Trimethylbenz(a)anthracene isomer **(iTMBA)**	$C_{21}H_{18}$	0.0022	aromatic HC
16	316, 444	Citrostediol	$C_{30}H_{52}O_2$	139.0	steroid
17	146, 378,	Ergosta-3,5,7,22-tetraene, (22E)-	$C_{28}H_{42}$	2872.0	steroid
18	189, 191	Diploptene	$C_{30}H_{50}$	1642.0	hopanoid
19	213, 329, 414	γ-Sitosterol	$C_{29}H_{50}O$	4640.0	steroid

20	215, 233, 401	Stigmastanol	$C_{29}H_{52}O$	1336.0	steroid
21	124, 229, 398	4-Campestene-3-one	$C_{28}H_{46}O$	352.0	steroid
22	189,218, 426	α-Amyrin	$C_{30}H_{50}O$	500.0	terpenoid
23	231, 343, 456	Unknown terpenoid	–	140.0	terpenoid
24	191, 396	4,4-Dimethylcholesterol	$C_{29}H_{50}O$	1143.0	steroid
25	189, 426	Lupeol	$C_{30}H_{50}O$	493.0	terpenoid
26	203, 218, 424	Olean-12-en-3-one	$C_{30}H_{48}O$	159.0	terpenoid
27	191, 396	4,4-Dimethylcholesterol	$C_{29}H_{50}O$	298.0	steroid
28	191	Unknown C_{35} homohopane	$C_{35}H_{62}$	301.0	terpenoid
29	191,470	18α-Olean-3β-ol, acetate	$C_{32}H_{54}O_2$	127.0	terpenoid
30	189, 426, 440	Homolupeol	$C_{31}H_{52}0$	531.0	terpenoid
31	395, 428	Lanost-8-en-3-ol, (3β)-	$C_{30}H_{52}O$	252.0	steroid
32	189, 207, 411, 442	Betulin	$C_{30}H_{50}O_2$	755.0	terpenoid

Table A1.8. Core H3, depth 0.50–0.75 m. Composition and content of identified steroid and terpenoid components of sample H3-69 by m/z 191. The labels on the mass fragmetogram are the peak numbers.

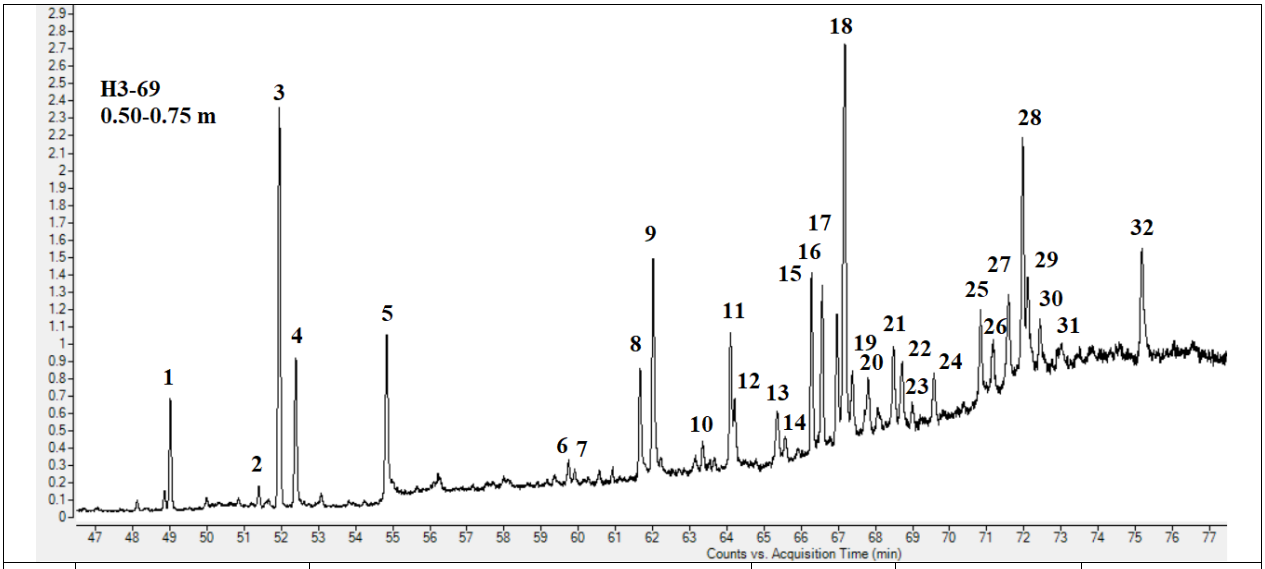

Peak No.	m/z	Component	Gross formula	Dry mass concentration (μg g^{-1})	Type
1	207, 263, 278	Anthra[2,3-b]furan-4,11-dione, 2,3-dihydro-3,6-dimethyl-	$C_{18}H_{14}O_3$	0.0015	aromatic HC
2	215,233,373, 388	Cholestanol	$C_{27}H_{48}O$	122.0	steroid
3	121, 219, 330	Pregnane-3,11,20-trione, (5β)-	$C_{21}H_{30}O_3$	430.0	steroid
4	202, 218	2-Benzylnaphthalene	$C_{17}H_{14}$	0.00051	aromatic hydrocarbon oil pollution
5	51, 96, 366	2-Pentacosanone	$C_{25}H_{50}O$	6.60	ketone
6	137, 177, 402	δ-Tocopherol	$C_{27}H_{46}O_2$	141.0	vitamin E
7	296, 341	Unknown compound	–	10.8	unknown
8	151, 191, 416	γ-Tocopherol	$C_{29}H_{48}O_2$	112.1	vitamin E
9	215,233,373, 388	β-Tocopherol	$C_{27}H_{48}O$	48.2	steroid
10	215,233,373, 388	Cholestanol	$C_{27}H_{48}O$	48.0	steroid
11	121, 191	C28 β -hopane	$C_{28}H_{48}$	129.0	terpenoid
12	203, 2017	24-Noroleana-4(23),12-diene, 3-methyl-, (3α)-	$C_{30}H_{48}$	32.0	terpenoid
13	315, 400	Campesterol	$C_{28}H_{48}O$	657.0	steroid
14	255, 270	Trimethylbenz(a)anthracene isomer (iTMBA)	$C_{21}H_{18}$	0.00082	aromatic HC
15	316, 444	Citrostediol	$C_{30}H_{52}O_2$	69.0	steroid
16	146, 378,	Ergosta-3,5,7,22-tetraene, (22E)-	$C_{28}H_{42}$	140.1	steroid
17	189, 191	Diploptene	$C_{30}H_{50}$	352.0	terpenoid
18	213, 329, 414	γ-Sitosterol	$C_{29}H_{50}O$	2706.0	steroid

19	215, 233, 401	Stigmastanol	$C_{29}H_{52}O$	628.0	steroid
20	124, 229, 398	4-Campestene-3-one	$C_{28}H_{46}O$	185.0	steroid
21	324, 385	Unknown aromatic compound	–	0.00033	unknown
22	189,218, 426	α-Amyrin	$C_{30}H_{50}O$	496.0	terpenoid
23	231, 343, 456	Unknown terpenoid	–	42.0	terpenoid
24	191, 396	4,4-Dimethylcholesterol	$C_{29}H_{50}O$	583.0	steroid
25	189, 426	Lupeol	$C_{30}H_{50}O$	123.0	terpenoid
26	203, 218, 424	Olean-12-en-3-one	$C_{30}H_{48}O$	161.0	terpenoid
27	191, 396	4,4-Dimethylcholesterol	$C_{29}H_{50}O$	214.0	steroid
28	191	Unknown C_{35} homohopane	$C_{35}H_{62}$	137.0	terpenoid
29	191,470	18α-Olean-3β-ol, acetate	$C_{32}H_{54}O_2$	41.0	terpenoid
30	189, 426, 440	Homolupeol	$C_{31}H_{52}0$	103.0	terpenoid
31	395, 428	Lanost-8-en-3-ol, (3β)-	$C_{30}H_{52}O$	72.1	steroid
32	189, 207, 411, 442	Betulin	$C_{30}H_{50}O_2$	432.3	terpenoid

Table A1.9. Core H3, depth 2.50–2.75 m. Composition and content of identified steroid and terpenoid components of sample H3-77 by m/z 191. The labels on the mass fragmetogram are the peak numbers.

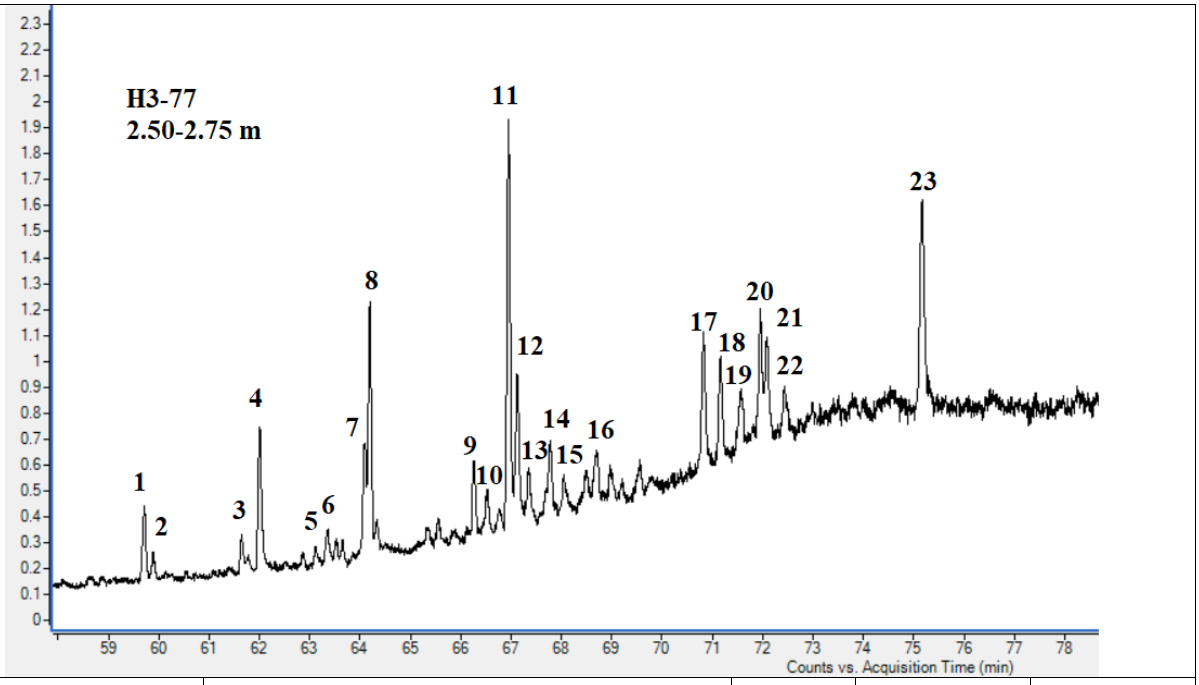

Peak No.	m/z	Component	Gross formula	Dry mass concentration (μg g^{-1})	Type
1	137, 177, 402	δ-Tocopherol	$C_{27}H_{46}O_2$	89.0	vitamin E
2	268, 296	Dinaphtho[2,3-b:1',2'-d]pyran-7-one **(DNP)**	$C_{21}H_{12}O_2$	0.00038	aromatic HC
3	151, 191, 416	γ-Tocopherol	$C_{29}H_{48}O_2$	118.0	vitamin E
4	151, 191, 416	β-Tocopherol	$C_{29}H_{48}O_2$	381.0	vitamin E
5	213,301, 386	Cholesterol	$C_{27}H_{46}O$	289.0	steroid
6	215,233,373, 388	Cholestanol	$C_{27}H_{48}O$	61.2	steroid
7	121, 191	C_{28} β -hopane	$C_{28}H_{48}$	412.0	terpenoid
8	191, 218, 410	Olean-13(18)-ene	$C_{30}H_{50}$	109.0	terpenoid
9	316, 444	Citrostediol	$C_{30}H_{52}O_2$	136.0	steroid
10	145, 426	Naphthalene, 5-(1-decylundecyl)-1,2,3,4-tetrahydro- 9 **(NDUT)**	$C_{31}H_{54}$	0.00011	aromatic HC
11	189, 191	Diploptene	$C_{30}H_{50}$	138.0	terpenoid
12	213, 329, 414	γ-Sitosterol	$C_{29}H_{50}O$	397.0	steroid
13	215, 233, 401	Stigmastanol	$C_{29}H_{52}O$	785.0	steroid
14	124, 229, 398	4-Campestene-3-one	$C_{28}H_{46}O$	285.0	steroid
15	217, 231, 414	3-oxo-Stigmastane	$C_{29}H_{50}O$	400.2	steroid
16	189,218, 426	α-Amyrin	$C_{30}H_{50}O$	790.0	terpenoid
17	189, 426	Lupeol	$C_{30}H_{50}O$	344.1	terpenoid
18	109, 273, 426	Friedelan-3-one	$C_{30}H_{50}O$	320.0	terpenoid
19	191, 396	4,4-Dimethylcholesterol	$C_{29}H_{50}O$	381.0	steroid
20	191	Unknown C_{35} homohopane	$C_{35}H_{62}$	119.0	terpenoid
21	191,470	18α-Olean-3β-ol, acetate	$C_{32}H_{54}O_2$	89.4	terpenoid
22	189, 207, 398	Betulinaldehyde	$C_{30}H_{48}O_2$	461.0	terpenoid
23	189, 207, 411, 442	Betulin	$C_{30}H_{50}O_2$	982.0	terpenoid

Table A1.10. Core H3, depth 4.50–4.75 m. Composition and content of identified steroid and terpenoid components of sample H3-85 by m/z 191. The labels on the mass fragmetogram are the peak numbers.

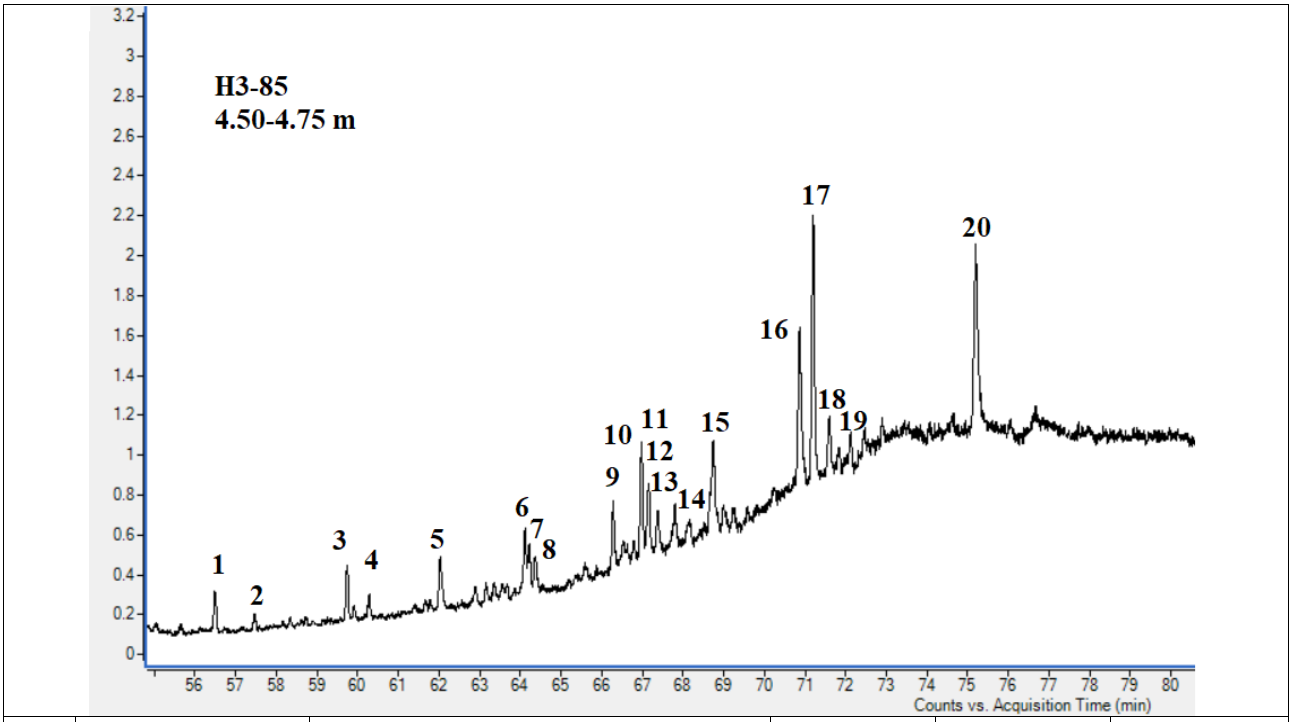

Peak No.	m/z	Component	Gross formula	Dry mass concentration (μg g^{-1})	Type
1	149, 191, 234	Unknown aromatic contaminant	–	8.2	contaminant
2	313, 373	12,24-Dioxocholan-3-yl acetate	$C_{26}H_{40}O_4$	3.0	steroid
3	137, 177, 402	δ-Tocopherol	$C_{27}H_{46}O_2$	6.0	vitamin E
4	189, 299	Unknown terpenoid	–	12.0	terpenoid
5	151, 191, 416	β-Tocopherol	$C_{29}H_{48}O_2$	25.0	vitamin E
6	121, 191	C_{28} β -hopane	$C_{28}H_{48}$	55.0	terpenoid
7	255, 270	Trimethylbenz(a)anthracene **(TMBA)**	$C_{21}H_{18}$	0.00012	aromatic HC
8	177, 191	C_{29} nor-hopane	$C_{29}H_{50}$	14.1	terpenoid
9	316, 444	Citrostediol	$C_{30}H_{52}O_2$	10.0	steroid
10	189, 191	Diploptene	$C_{30}H_{50}$	12.0	terpenoid
11	213, 329, 414	γ-Sitosterol	$C_{29}H_{50}O$	7.0	steroid
12	215, 233, 401	Stigmastanol	$C_{29}H_{52}O$	67.0	steroid
13	124, 229, 398	4-Campestene-3-one	$C_{28}H_{46}O$	23.0	steroid
14	217, 231, 414	3-oxo-Stigmastane	$C_{29}H_{50}O$	29.0	steroid
15	189,218, 426	α-Amyrin	$C_{30}H_{50}O$	115.0	terpenoid
16	189, 426	Lupeol	$C_{30}H_{50}O$	75.0	terpenoid
17	109, 273, 426	Friedelan-3-one	$C_{30}H_{50}O$	129.0	terpenoid
18	191, 396	4,4-Dimethylcholesterol	$C_{29}H_{50}O$	32.0	steroid
19	191,470	18α-Olean-3β-ol, acetate	$C_{32}H_{54}O_2$	9.0	terpenoid
20	189, 207, 411, 442	Betulin	$C_{30}H_{50}O_2$	141.0	terpenoid

Table A1.11. Core H3, depth 4.75–5.00 m. Composition and content of identified steroid and terpenoid components of sample H3-86 by m/z 191. The labels on the mass fragmetogram are the peak numbers.

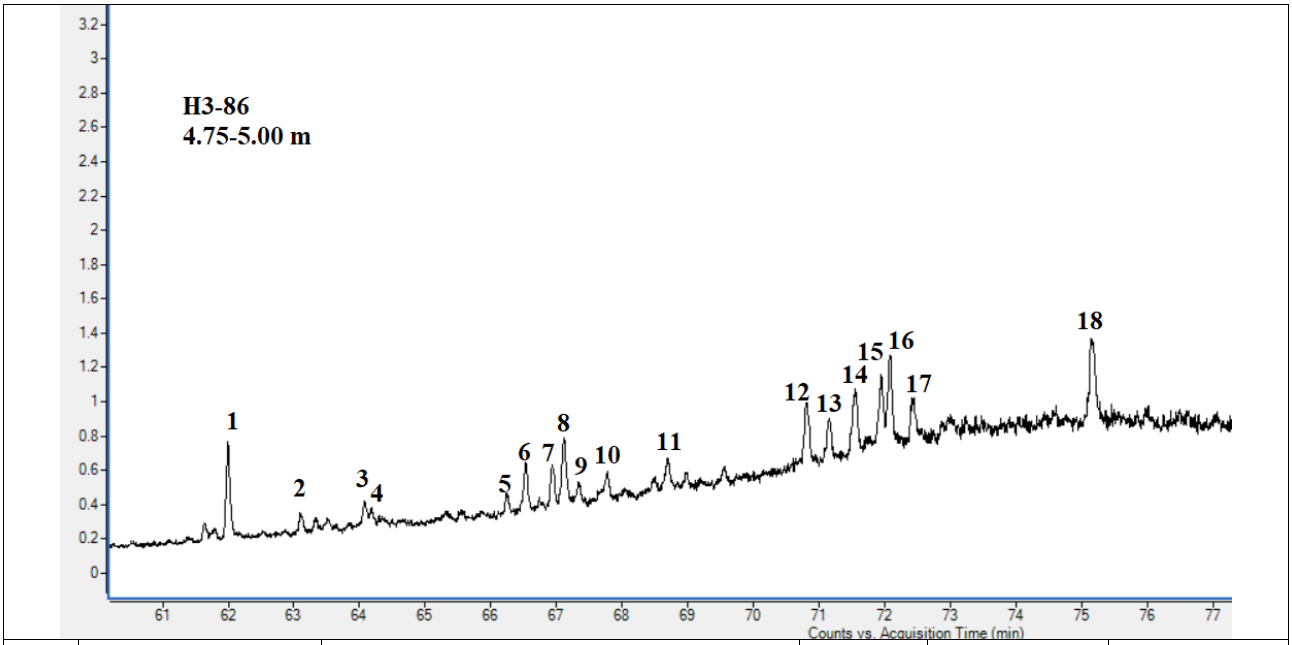

Peak No.	m/z	Component	Gross formula	Dry mass concentration (μg g^{-1})	Type
1	151, 191, 416	β-Tocopherol	$C_{29}H_{48}O_2$	33.0	vitamin E
2	213, 301, 353, 386	Cholesterol	$C_{27}H_{46}O$	111.0	steroid
3	121, 191	C_{28} β -hopane	$C_{28}H_{48}$	99.0	terpenoid
4	255, 270	Trimethylbenz(a)anthracene **(TMBA)**	$C_{21}H_{18}$	0.00019	aromatic HC
5	316, 444	Citrostediol	$C_{30}H_{52}O_2$	18.0	steroid
6	146, 378,	Ergosta-3,5,7,22-tetraene, (22E)-	$C_{28}H_{42}$	143.1	terpenoid
7	189, 191	Diploptene	$C_{30}H_{50}$	53.3	terpenoid
8	213, 329, 414	γ-Sitosterol	$C_{29}H_{50}O$	328.0	steroid
9	215, 233, 401	Stigmastanol	$C_{29}H_{52}O$	155.0	steroid
10	124, 229, 398	4-Campestene-3-one	$C_{28}H_{46}O$	59.0	steroid
11	189,218, 426	α-Amyrin	$C_{30}H_{50}O$	163.0	terpenoid
12	189, 426	Lupeol	$C_{30}H_{50}O$	64.3	terpenoid
13	109, 273, 426	Friedelan-3-one	$C_{30}H_{50}O$	42.0	terpenoid
14	191, 396	4,4-Dimethylcholesterol	$C_{29}H_{50}O$	87.0	steroid
15	191	Unknown C_{35} homohopane	$C_{35}H_{62}$	27.0	terpenoid
16	191,470	18α-Olean-3β-ol, acetate	$C_{32}H_{54}O_2$	45.0	terpenoid
17	189, 426, 440	Homolupeol	$C_{31}H_{52}O$	132.0	terpenoid
18	189, 207, 411, 442	Betulin	$C_{30}H_{50}O_2$	224.0	terpenoid

Appendix 2

Table A2.1. Structures of identified organic compounds in the peat of the Ob Fen. In the second and third columns, a shaded cell indicates that the compound is absent from one core (H2 or H3).

No.	H2	H3	Component	Structural formula
1			δ-Tocopherol	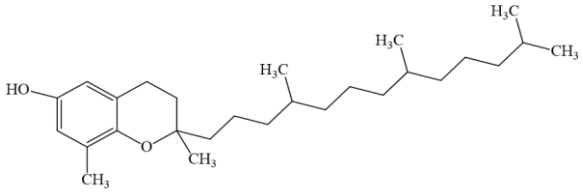
2			γ-Tocopherol	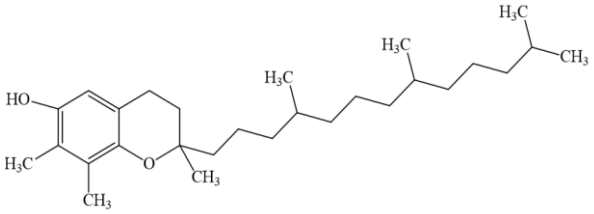
3			β-Tocopherol	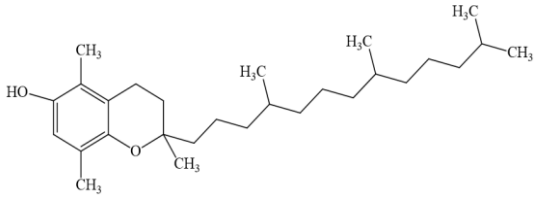
4			Cholestanol	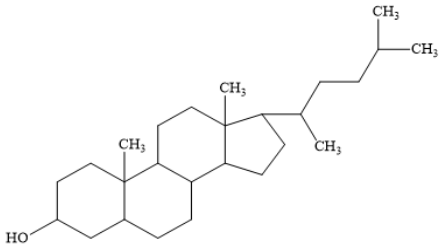
5			Trimethylbenz[a]anthracene **(TMBA)**	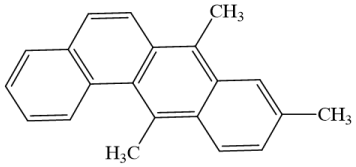
6			Campesterol	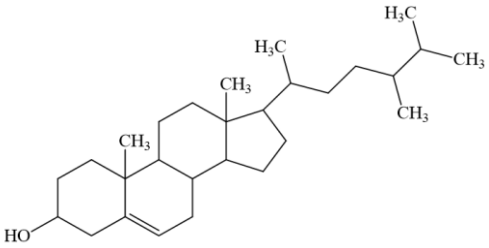

No.	H2	H3	Component	Structural formula
7			Citrostediol	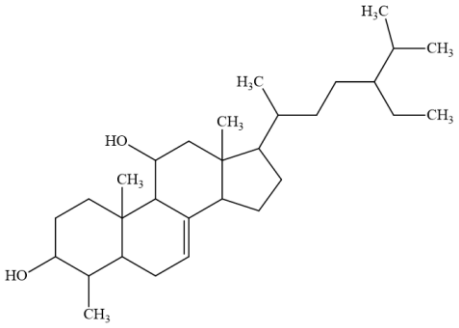
8			Ergosta-3,5,7,22-tetraene, (22E)-	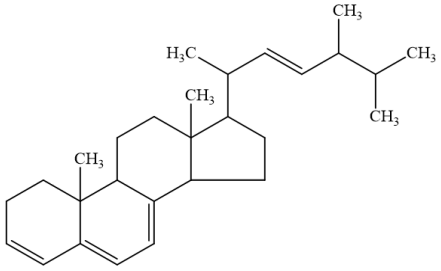
9			Diploptene	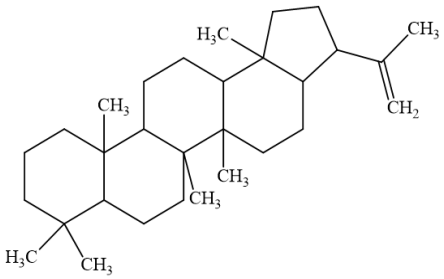
10			γ-Sitosterol	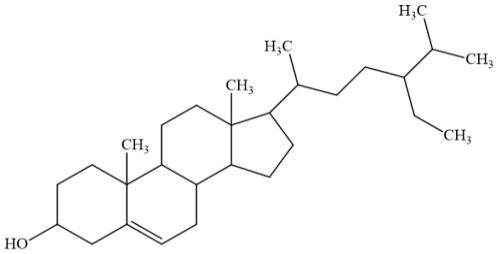
11			Stigmastanol	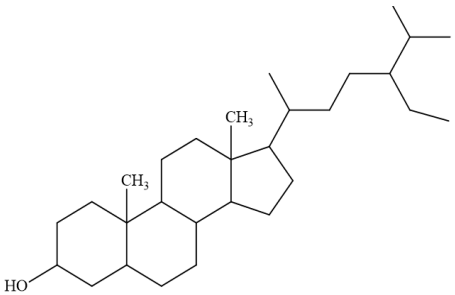

No.	H2	H3	Component	Structural formula
12			4-Campestene-3-one	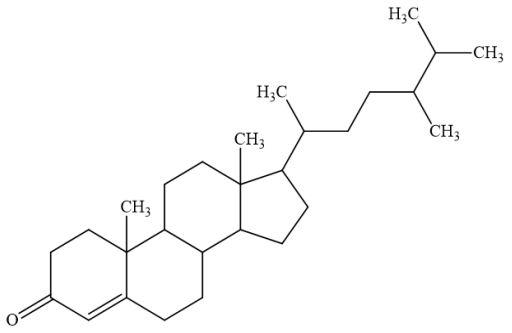
13			3-oxo-Stigmastane	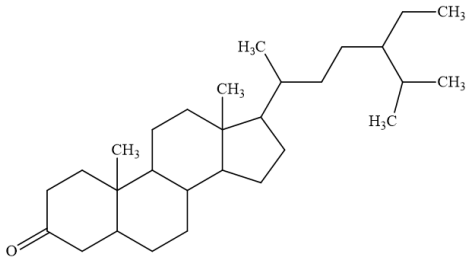
14			α-Amyrin	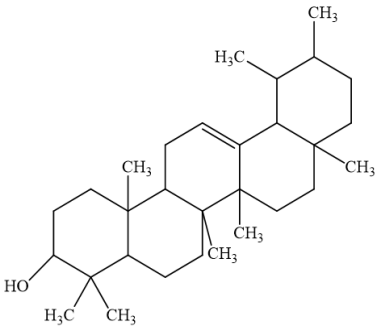
15			γ-Sitostenone	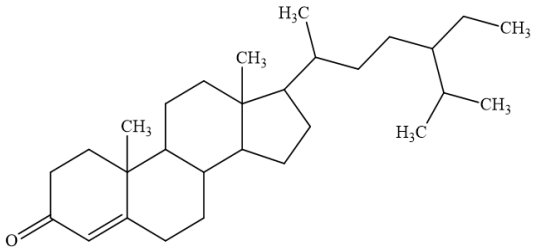
16			Lupeol	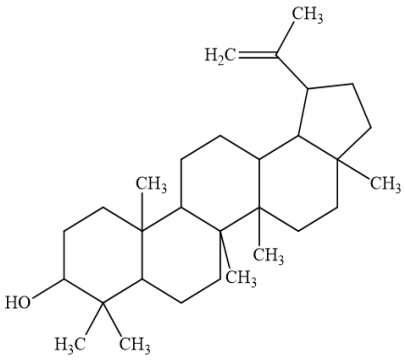

No.	H2	H3	Component	Structural formula
17			4,4-Dimethylcholesterol	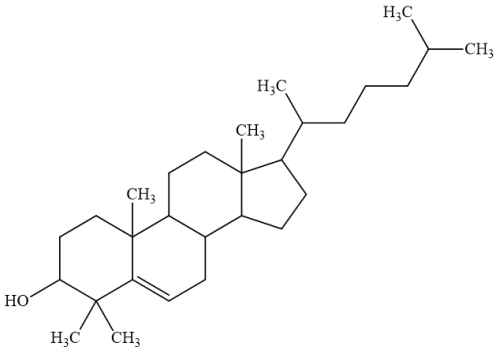
18			Betulin	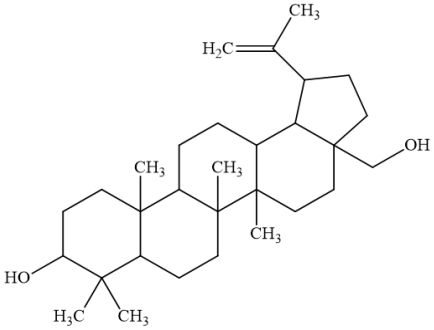
19			C_{28} 17β21β hopane	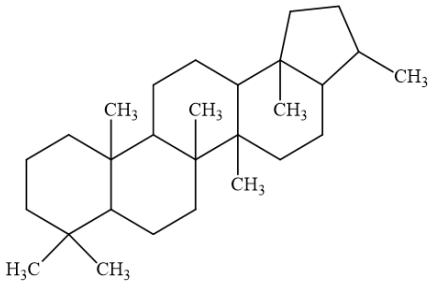
20			28-Nor-Δ12, Δ18-oleandien-3-ol	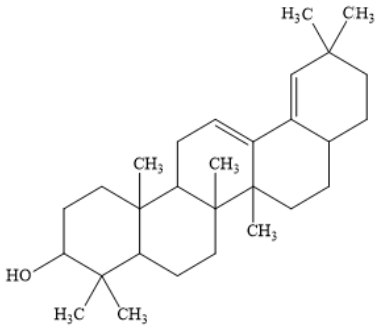
21			Betulinaldehyde	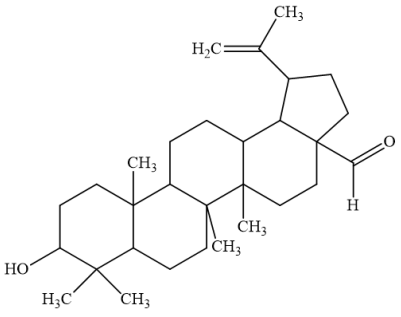

No.	H2	H3	Component	Structural formula
22			(3β,5β)-Cholestan-3-ol	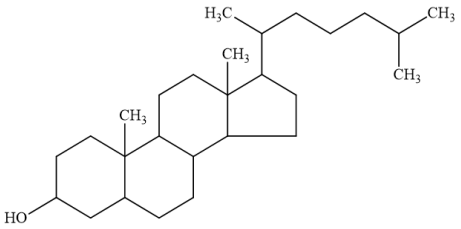
23			Ergosta-5,7,9(11),22-tetraen-3-ol, (3β,22E)-	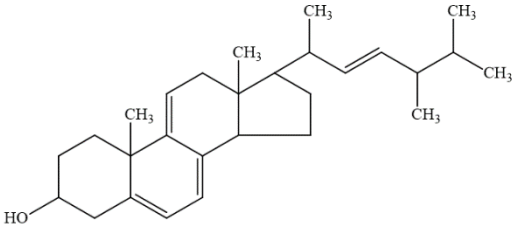
24			Citrostediol	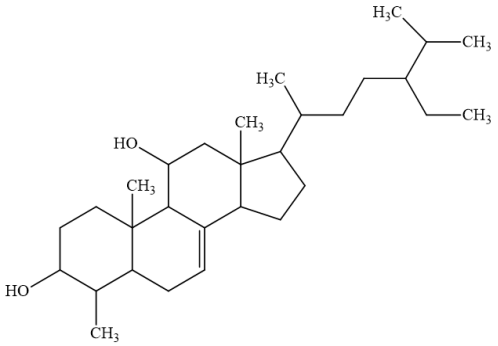
25			Campest-4-en-3-one	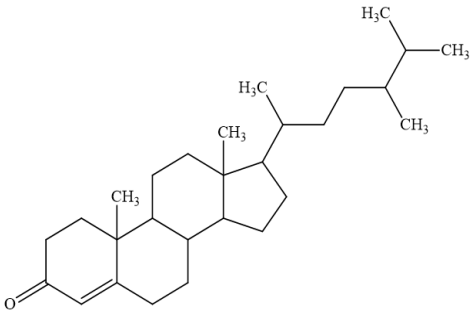
26			4,4-Dinorlupan-4-one-28-carboxylic acid, 3β-methyl-, methyl ester	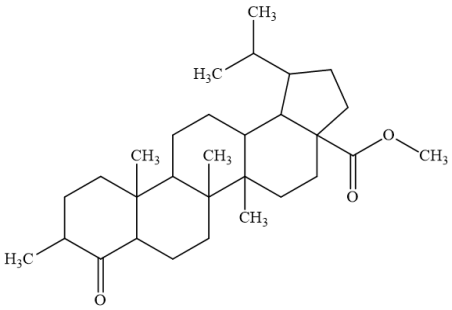

No.	H2	H3	Component	Structural formula
27			9,19-Cyclo-25,26-epoxyergostan-3-ol, 4,4,14-trimethyl-, acetate	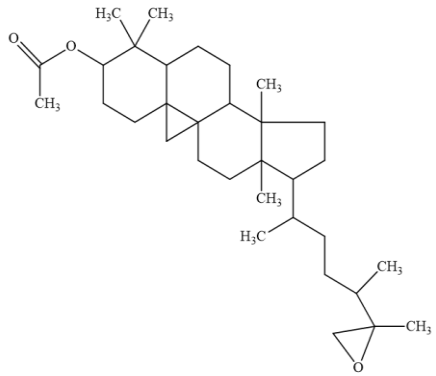
28			18α-Olean-3β-ol, acetate	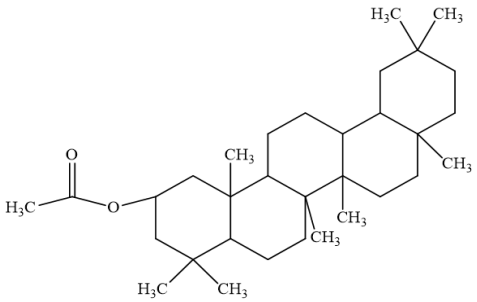
29			Dinaphtho[2,3-b:1',2'-d]pyran-7-one **(DNP)**	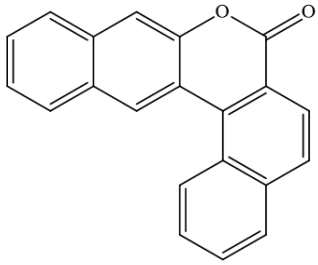
30			Olean-13(18)-ene	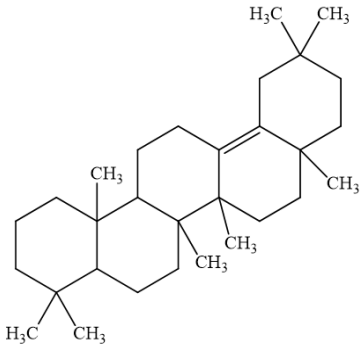
31			Naphthalene, 5-(1-decylundecyl)-1,2,3,4-tetrahydro- 9 **(NDUT)**	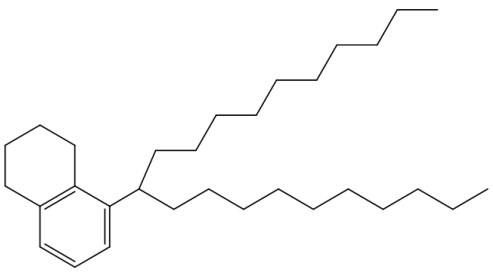

No.	H2	H3	Component	Structural formula
32			17α,21β-28,30-Bisnorhopane	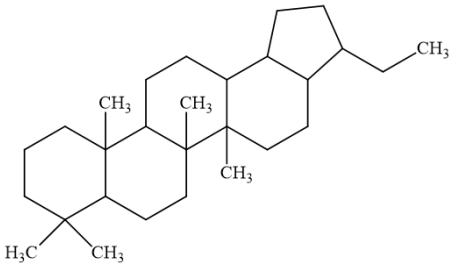
33			Friedelan-3-one	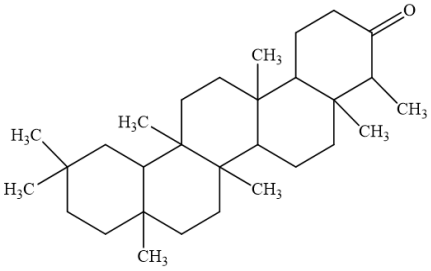
34			4,4-Dinorlupan-4-one-28-carboxylic acid, 3β-methyl-, methyl ester	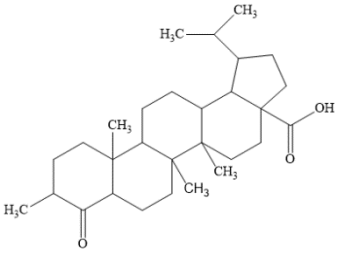
35			Anthra[2,3-b]furan-4,11-dione, 2,3-dihydro-3,6-dimethyl-	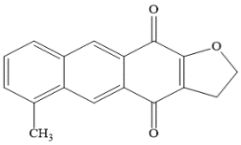
36			Tridecyl decanoate	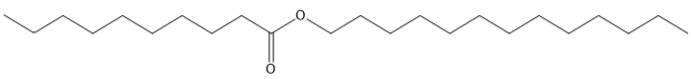
37			2-Benzylnaphthalene	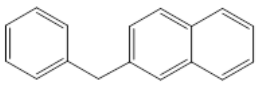
38			2-Pentacosanone	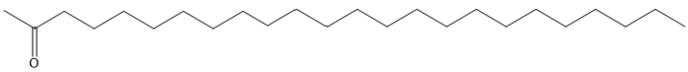
39			24-Noroleana-4(23),12-diene, 3-methyl-, (3α)-